J Solid State Electrochem (2012) 16:2751–2758
DOI 10.1007/s10008-012-1694-7

ORIGINAL PAPER

Synthesis and high electrochemical performance of polyaniline/MnO_2-coated multi-walled carbon nanotube-based hybrid electrodes

Ki-Seok Kim · Soo-Jin Park

Received: 17 September 2011 / Revised: 13 February 2012 / Accepted: 14 February 2012 / Published online: 3 March 2012

Abstract Multi-layered electrodes which consist of polyaniline (PANI)/manganese dioxide (MnO_2)-multi-walled carbon nanotubes (MWNTs) are prepared as the electrode materials for supercapacitors. MnO_2-MWNTs are made by the in situ direct coating method to deposit MnO_2 onto MWNTs; the core/shell structure of multi-layered fibrous electrodes can also be obtained by PANI coating onto the MnO_2-MWNTs. The effect of PANI coating on the electrochemical performance and cyclic stability of MnO_2-MWNTs is investigated. From the cyclic voltammograms, the PANI/MnO_2-MWNTs show remarkably enhanced specific capacitance and cycle stability compared to MnO_2-MWNTs, where the highest specific capacitance (350 F/g) is obtained at a current density of 0.2 A/g for the PANI/MnO_2-MWNTs as compared to 92 F/g for pristine MWNTs and 306 F/g for MnO_2-MWNTs. This indicates that the improved electrochemical performance of PANI/MnO_2-MWNTs is due to the enhanced electrical properties by nano-scale-coated MnO_2 onto MWNTs and the PANI coating that leads to the increased cycle stability by delaying the dissolution of MnO_2 during charge/discharge tests.

Keyword Multi-walled carbon nanotubes · Manganese oxide · Polyaniline · Electrochemical performance

Introduction

A supercapacitor, which is also known as an electrochemical capacitor, is a charge storage device between the traditional electrostatic capacitor and the rechargeable battery. It has been used as an energy storage system for portable electronic devices, backup power sources, and hybrid electric vehicles due to its high power, energy density, and long cycle life [1–3]. As the electrode for the supercapacitor, carbon materials, transition metal oxides (TMs), and a combination of conducting polymers (CPs) [4] and hybrid systems, consisting of carbon/TMs [5], carbon/CPs [6], TMs/CPs [7], or all three phases, i.e., carbon/TMs/CPs [8], are commonly utilized and hence have been studied for their energy storage capacities to be improved using their synergistic effect.

Recently, much research has been done to design new electrode materials for supercapacitors to enhance their electrochemical behaviors. Ruthenium oxide has a specific capacitance as high as 720 F/g and exhibits excellent cycle life stability in aqueous electrolytes. However, its high cost limits potential applications [9]. Therefore, many research interests have been prompted to focus on other transition metal oxides and conducting polymers. In this regard, manganese oxide is one of the most attractive candidates for electrochemical capacitor electrode materials due to its environmental friendliness and low cost [10, 11], whereas one of the major challenges with manganese oxide is its low electrical conductivity. Indeed thin MnO_2 films exhibited an electrical conductivity of about ~700 F/g. However, the specific capacitance gradually decreases with increasing film thickness, and the reported values are usually in the range from 100 to 250 F/g [12]. Thus, many approaches have been taken to overcome this disadvantage through synthesizing specific nanostructures [13] or composites with conducting materials, such as carbon nanotubes and conducting polymers [14, 15]. Of these, conducting polymers have also been widely utilized as electrode materials for supercapacitors owing to their good electrical conductivity

K.-S. Kim · S.-J. Park (✉)
Department of Chemistry, Inha University,
Incheon 402-751, Korea
e-mail: sjpark@inha.ac.kr

and large pseudocapacitance that are comparable to those of transition metals. Among the conductive polymers, polyaniline (PANI) is considered to be the most promising electrode material for supercapacitors due to its excellent capacity for energy storage, good processability, high conductivity, low cost, and environmental stability [16–18].

Many studies have recently been carried out on the electrochemical performance of manganese oxide/carbon materials to improve their electrical properties. However, there has been a limited amount of work published on the electrochemical performance of multi-phase materials prepared from conducting polymer/transition metal/carbon materials for supercapacitor electrodes.

Therefore, in the present study, multi-layered electrodes in the form of conducting polymer/transition metal/carbon nanotubes were prepared in two steps: (1) manganese oxide was coated in nano-scaled thickness onto multi-walled carbon nanotubes (MWNTs) by a direct coating method by the reduction of $KMnO_4$ and (2) PANI was further deposited onto manganese oxide-coated MWNTs (MnO_2-MWNTs) using oxidation polymerization. The synergistic effect, resulting from the multi-layered structures and pseudocapacitive reaction, on the electrochemical properties of the PANI/MnO_2-MWNTs is discussed.

Materials and methods

Materials

MWNTs produced by chemical vapor deposition process were obtained from Nanosolution Co. (Korea). The properties of the MWNTs may be summarized as follows: purity >95% (C, 96 %), diameter 10 to 25 nm, and length 25 to 50 μm. MWNTs were used after conventional acid treatment using a sulfuric acid and nitric acid (3:1, *v*/*v*) mixture. Aniline and ammonium persulfate (APS) were obtained from Aldrich. Potassium permanganate ($KMnO_4$) was supplied by Sam Chun Chem. (Korea). The citric acid and all other organic solvents used in this study were of analytical grade and were used without further purification.

Synthesis of MnO_2-MWNTs

First, 1 g of MWNTs was acid-treated with 200 ml of a sulfuric acid and nitric acid mixture (3:1, *v*/*v*) under sonication for 2 h and was then reacted for 6 h at 80 °C under stirring. Acid-treated MWNTs (A-MWNTs) were washed with water until a pH level of 7.0 was attained, after which the washed sample was filtered and dried at 100 °C.

Then, 0.5 g of A-MWNTs was mixed with 100 ml of 0.2 M $KMnO_4$ solution in a flask. The solution mixture was then refluxed at 140 °C with stirring for 12 h. After the reaction, the mixture was filtered and washed with distilled water several times to remove the residual $KMnO_4$. Subsequently, the filter cake was redispersed in 200 ml of deionized water followed by the addition of 10 ml of 1 M citric acid and then maintained at 160 °C for 12 h under vigorous agitation using a magnetic stirrer during the whole course. A condenser was fitted to the reactor to prevent liquid loss by evaporation. Finally, the composite products were obtained through filtering, purifying with water, and drying processes. Consequently, the resulting samples were MnO_2-MWNTs.

Synthesis of PANI/MnO_2-MWNTs

First, 0.1 g of MnO_2-MWNTs was dispersed in 100 ml of 1 M HCl solution with the assistance of ultrasonication for 1 h. Then, 5 ml of the aniline monomer was added to the MnO_2-MWNTs solution with constant stirring. After that, 100 ml of 0.1 M APS solution was added dropwise to the above solution for 30 min to initiate oxidation polymerization. The reaction was continued for 24 h at 0 to 5 °C. Then, the final product was washed with water and acetone. The remaining powder was dried in a vacuum oven at 80 °C for 24 h. The scheme for PANI/MnO_2-MWNTs preparation is presented in Fig. 1.

Measurements

The morphologies of MWNTs, MnO_2-MWNTs, and PANI/MnO_2-MWNTs were observed by scanning electron microscopy (SEM, S-4200, Hitachi).

The thermal properties of MWNTs, MnO_2-MWNTs, and PANI/MnO_2-MWNTs were measured using thermogravimetric analyses (TGA, Du-Pont TGA-2950 analyzer) from 30 to 750 °C at a heating rate of 10 °C/min in a nitrogen atmosphere.

The structural characteristics of MWNTs, MnO_2-MWNTs, and PANI/MnO_2-MWNTs were confirmed by X-ray diffraction (XRD, Rigaku D/Max 2200 V) at 40 kV and 40 mA using Cu Kα radiation. The XRD patterns were obtained in 2θ range between 5° and 70° at a scanning rate of 2°/min.

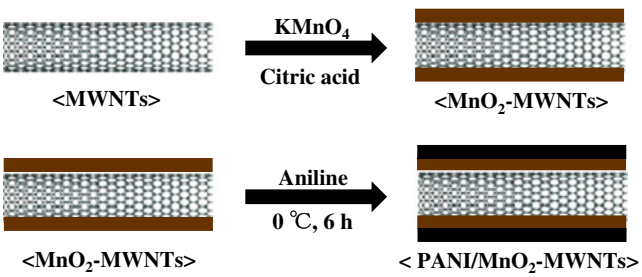

Fig. 1 A scheme for the preparation of MnO_2-MWNTs and PANI/MnO_2-MWNTs

Surface characterization of MWNTs, MnO_2-MWNTs, and PANI/MnO_2-MWNTs was carried out using X-ray photoelectron spectroscopy (XPS, K-Alpha) using a VG Scientific ESCALAB MK-II spectrometer equipped with MgKα (1,253.6 eV) X-ray source and a high-performance multichannel detector operated at 200 W.

Electrochemical performances of MWNTs, MnO_2-MWNTs, and PANI/MnO_2-MWNTs were characterized using a three-electrode electrochemical cell. The three-electrode cell consists of a Pt wire as a counter electrode, an Ag/AgCl reference electrode, and SUS mesh coated with the sample as the working electrode. For a working electrode, each sample, carbon black, and PVDF (70:20:10, *w*/*w*) were mixed and dispersed in NMP. The slurry mixture was then coated onto SUS mesh, which was dried at 100 °C for 12 h. Cyclic voltammetry measurements were carried out on an IviumStat instrument in 0.5 M Na_2SO_4 solution at a scan rate of 2 to 50 mV/s in a voltage range of −0.2 to 1.0 V. Galvanostatic charge/discharge curves were measured at a current density of 0.2 A/g.

Results and discussion

Characterization of PANI/MnO_2-MWNTs

Figure 2 shows the TGA thermogram of MWNTs, MnO_2-MWNTs, and PANI/MnO_2-MWNTs. It can be seen that MWNTs exhibit higher thermal stability (weight loss, about 5%) of up to 750 °C with partial weight loss. However, the thermogram of MnO_2-MWNTs is visibly different. MnO_2-MWNTs exhibit a gradual weight loss (14%) up to melting point (535 °C), and then the total weight loss with second degradation is about 20%. The thermal degradation of PANI/MnO_2-MWNTs is a three-step weight loss process. The first weight loss at approximately 100 °C is attributed to the loss of residual solvents and the weight loss from 220 to 310 °C results from the elimination of HCl as a dopant. The third weight loss, from approximately 400 to 600 °C, corresponds to the thermal decomposition of the PANI and MnO_2 [19, 20].

The structural features of MWNTs, MnO_2-MWNTs, and PANI/MnO_2-MWNTs are determined using XRD (shown in Fig. 3). The pristine MWNTs revealed reflections corresponding to *d*(002) and *d*(100) planes of the crystalline graphite-like materials at 2θ=26° and 43°, respectively [6], whereas five peaks in MnO_2-MWNTs are detected at 2θ= 18°, 36°, 38°, 44°, 56°, and 64°, corresponding to *d*(131), *d*(230), *d*(300), *d*(160), and *d*(242) of MnO_2 coated onto MWNTs (Joint Committee on Powder Diffraction Standards card no. 14-0644). These results indicate that nano-scaled MnO_2 was successfully deposited on the MWNTs. In the PANI/MnO_2-MWNTs, two broad peaks can be observed at 2θ=20° and 25°, resulting from the periodicity parallel and perpendicular to the polymer chain [21]. However, the main peaks of MWNTs and MnO_2 overlapped with each other and therefore disappeared after PANI coating.

Recently, the composites between electrical materials, such as carbons and conductive polymers, and MnO_2 have been studied by many researchers to improve the electrical properties of neat MnO_2 [22, 23]. Figure 4 shows SEM images of the pristine MWNTs, MnO_2-MWNTs, and PANI/MnO_2-MWNTs. The pristine MWNTs (Fig. 4a) are in an aggregated form and have a smooth surface where the diameters are approximately 20 to 40 nm and the lengths are of a few micrometers. Compared to pristine MWNTs, MnO_2-MWNTs exhibit a rougher surface and a thicker diameter due to the MnO_2 coating. The diameter of the MnO_2-MWNTs is approximately 30 to 50 nm, indicating

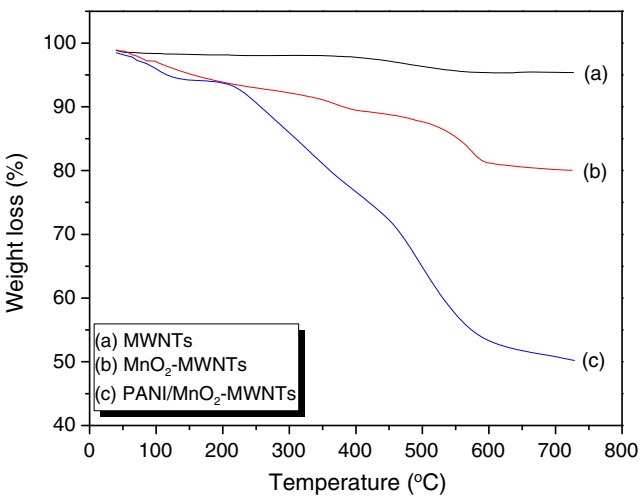

Fig. 2 TGA thermogram of pristine MWNTs, MnO_2-MWNTs, and PANI/MnO_2-MWNTs

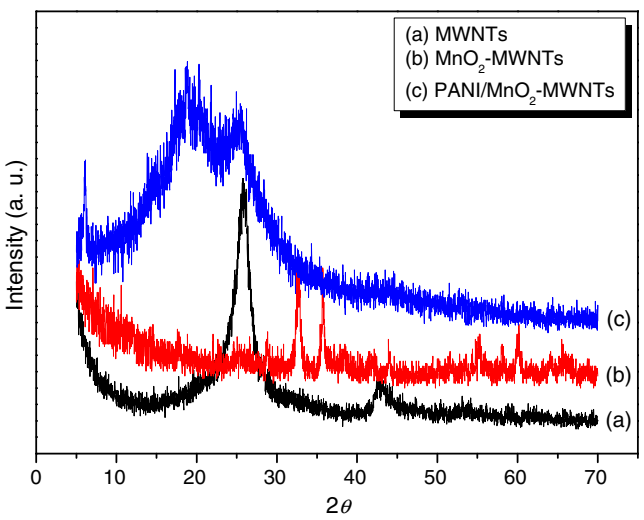

Fig. 3 XRD patterns of pristine MWNTs, MnO_2-MWNTs, and PANI/MnO_2-MWNTs

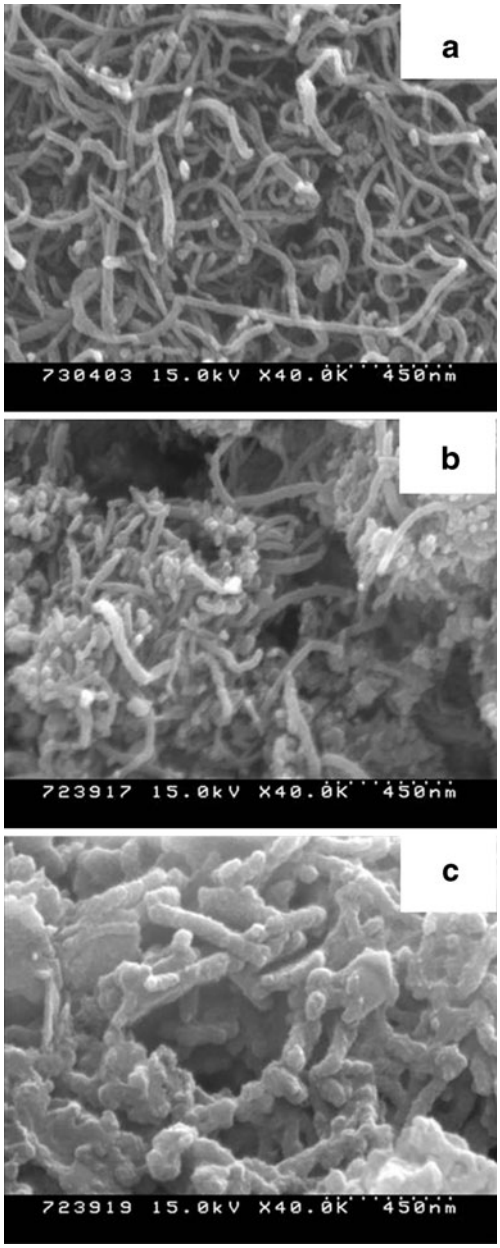

Fig. 4 SEM images of **a** pristine MWNTs, **b** MnO_2-MWNTs, and **c** PANI/MnO_2-MWNTs

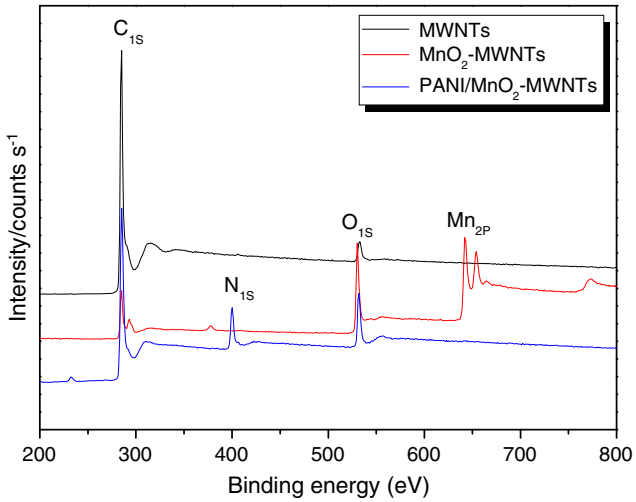

Fig. 5 XPS wide scan of pristine MWNTs, MnO_2-MWNTs, and PANI/MnO_2-MWNTs

that the MnO_2 layer is about 10 nm, although the diameter is locally decreased by the strong oxidation effect. To improve the electric and electrochemical properties of MnO_2, MWNTs were used as the substrate for the nano-scaled MnO_2 layer, and nano-scale coating of MnO_2 onto MWNTs leads to improved electrical properties and an increase in the specific surface area of MnO_2. In addition, it can also provide a synergistic effect not found in either MnO_2 or MWNTs alone. In general, the pseudocapacitive reaction of manganese dioxide occurs at its surface, presenting a nano-scale layer of MnO_2 onto MWNTs that can achieve high specific capacity and good high-rate capability. Furthermore, in the PANI/MnO_2-MWNTs, the thickness of MnO_2-MWNTs is also increased with the coating of PANI. As the diameter of the PANI/MnO_2-MWNTs is about 60 to 80 nm, this means that the PANI layer is about 30 nm.

XPS analysis of PANI/MnO_2-MWNTs

The elemental composition of MWNTs, MnO_2-MWNTs, and PANI/MnO_2-MWNTs was confirmed by XPS analysis (shown in Fig. 5 and Table 1). The survey scans, in the 200- to 800-eV binding energy range, confirm that acid-treated MWNTs mainly consist of carbon (285 eV) and oxygen (530 eV). Compared to MWNTs, with the incorporation of MnO_2, MnO_2-MWNTs exhibit peaks for MnO_2 (approximately 640 to 650 eV) as well as for carbon and oxygen groups, where the MnO_2 content is about 13.1 % (shown in Table 1). After further PANI coating, as expected, a nitrogen group (about 400 eV; content, 11 %) was newly formed on the PANI/MnO_2-MWNTs surface, whereas only a very small amount of MnO_2 was detectable [over the depth (> 10 nm) of analysis]. Consequently, the thickness of the PANI layer is estimated to be over 10 nm, as the SEM images suggest (Fig. 4). From the XPS results, the nano-scale-coated MnO_2 layer and the presence of high nitrogen content in the multi-layered composites could

Table 1 The element components of MWNTs, MnO_2-MWNTs, and PANI/MnO_2-MWNTs

	C (%)	O (%)	Mn (%)	N (%)
MWNTs	95.24	4.04	–	0.72
MnO_2-MWNTs	56.29	29.39	13.06	1.26
PANI/MnO_2-MWNTs	78.21	10.65	0.14	11.0

influence the electrochemical performance of the PANI/MnO_2-MWNTs by a pseudocapcitance reaction and subsequently increase the wettability of the electrolyte.

MnO_2-MWNTs are further examined to determine the oxygen anion content and the oxidation state of the Mn cations in manganese dioxide coated onto MWNTs. Mn_{2P} and O_{1S} spectra form MnO_2-MWNTs are shown in Fig. 6, and the valence of Mn cations is investigated using the Mn_{2P} spectrum. In Fig. 6a, the $Mn_{2P3/2}$ and $Mn_{2P1/2}$ binding energy peaks are located at 642.1 and 653.9 eV, respectively. The peak width between $Mn_{2P3/2}$ and $Mn_{2P1/2}$ is 11.8 eV, indicating an Mn valence of 4^+ and/or 3^+. The O_{1S} spectrum consists of two major components, namely, MnO_2 (Mn^{4+}) and MnOOH oxide (Mn^{3+}), and one minor component, the residual water. Of the two major components, the amount of MnO_2 is greater than that of MnOOH. These results provide useful information regarding the state of oxygen bonding, hydration of the oxide nanocrystals, and the valence of manganese cations, which can help to understand the capacitance mechanism as a fraction of the reaction sites accessible to the faradic process [24].

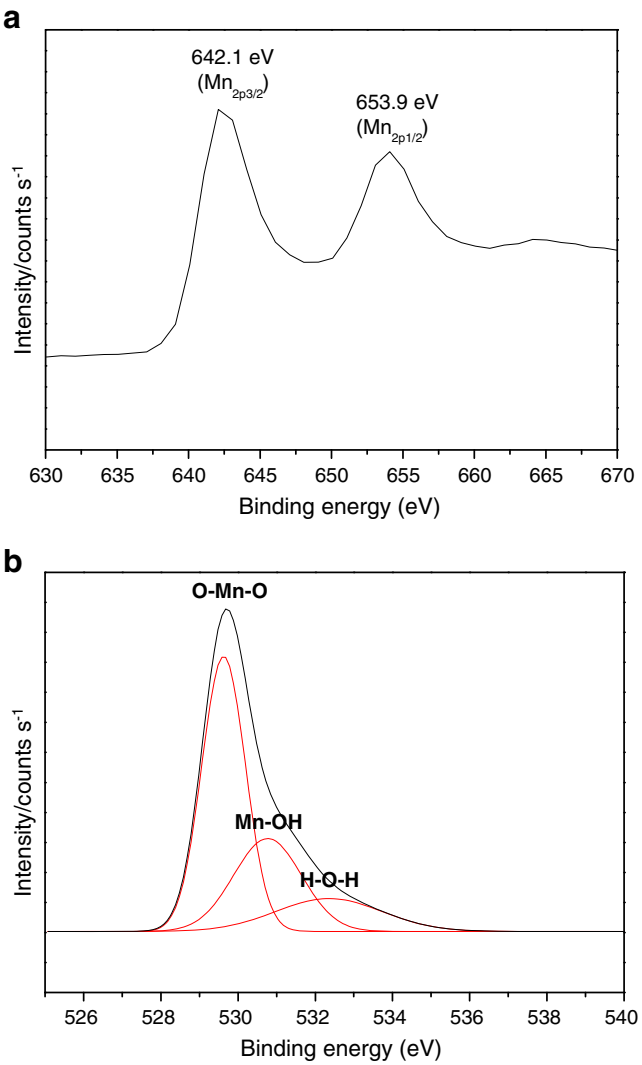

Fig. 6 Mn_{2p} peak **a** and peak fitting of O_{1S} **b** of MnO_2-MWNTs

Electrochemical performance of PANI/MnO_2-MWNTs

One-dimensional (1D) nanostructured materials provide short transport/diffusion path lengths for both ions and electrons, leading to faster kinetics and larger specific surface areas, resulting in high charge/discharge capacities [25]. In this work, cyclic voltammetry measurements were carried out to determine the electrochemical performance of MWNTs, MnO_2-MWNTs, and PANI/MnO_2-MWNTs at 5 mV/s in a 0.5-M Na_2SO_4 electrolyte solution. The CV curves of MWNT-, MnO_2-MWNT-, and PANI/MnO_2-MWNT-based electrodes are presented in Fig. 7a. It is clear that the current density of pristine MWNTs is lower than

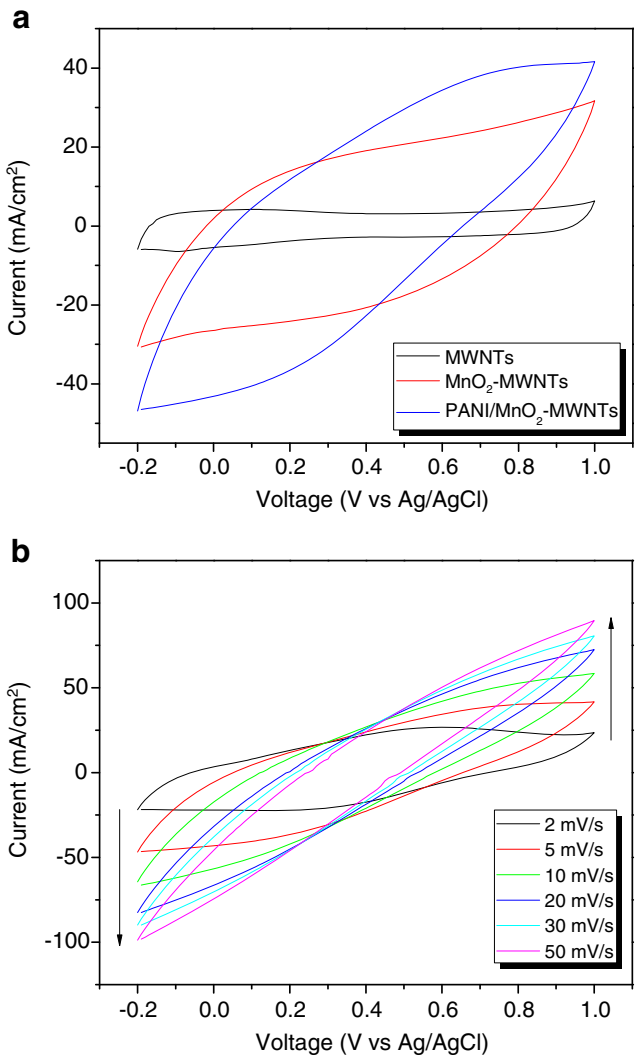

Fig. 7 Cyclic voltammetry of **a** pristine MWNTs, MnO_2-MWNTs, and PANI/MnO_2-MWNTs at 5 mV/s and **b** PANI/MnO_2-MWNTs with different scan rates (2 to 50 mV/s) in 0.5 M Na_2SO_4 solution

those of the multi-layered composite samples. However, it can be significantly improved with the incorporation of nano-scale-coated MnO_2, giving a larger current density. Furthermore, the current density of MnO_2-MWNTs is also increased by the application of PANI layers. The improved electrochemical performance of PANI/MnO_2-MWNTs is related to the formation of nano-scaled MnO_2 layers onto MWNTs, which provides a high specific surface area and enhanced electrical property of MnO_2 compared to the general particles, leading to easy and rapid penetration of electrolyte ions. Furthermore, the presence of polar nitrogen groups by PANI coating enhances the wettability between the electrode and electrolyte during charge–discharge, and the highly pseudocapacitive reaction is caused by the MnO_2 and nitrogen groups [26].

The rate capability for the supercapacitor is an important factor. To determine the rate capability of the electrode, CV measurements of PANI/MnO_2-MWNTs were performed in the range from 2 to 50 mV/s as shown in Fig. 7b. When the scan rate was increased up to 10 mV/s, the shape of the CV curve remained stable, and the current density was significantly increased without deformation of the CV curves, indicating a good rate capability of PANI/MnO_2-MWNTs. However, the CV curves are deformed at a high scan rate of over 10 mV/s due to the resistance of the electrodes.

It is well known that MnO_2 is one of the most promising electrode materials for supercapacitors due to its excellent capacitive performance in the aqueous electrolytes. The charging mechanism of MnO_2 is described by the following reaction [27]:

$$MnO_2 + B^+ + e^- \rightleftarrows MnO_2B \quad (1)$$

where $B^+ = Li^+$, Na^+, K^+, H^+. Equation 1 indicates that a large surface area and high ionic and electronic conductivity of the electrode material are necessary in order to utilize the high theoretical specific capacitance (theoretic value, 1,380 F/g) of MnO_2 [28].

Figure 8 shows the charge/discharge curves of the MWNTs, MnO_2-MWNTs, and PANI/MnO_2-MWNTs. As shown in Fig. 8, at a current density of 0.2 A/g, MWNTs are in an ideal triangular shape with a small ohmic drop at the beginning of the discharge, and this reveals that MWNTs possess excellent capacitive behaviors [29]. However, MnO_2-MWNTs and PANI/MnO_2-MWNTs exhibit a large ohmic drop compared to that of MWNTs, presenting the high equivalent series resistance (ESR) in the interface of multi-layered electrodes. Although the ESR of the multi-layered electrodes is high, their charge/discharge duration is significantly increased with the incorporation of MnO_2 and further PANI layers. From the charge–discharge curve, the

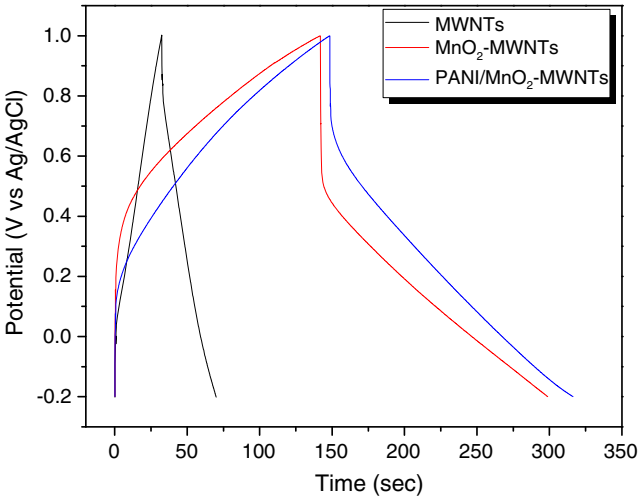

Fig. 8 Charge–discharge behaviors of pristine MWNTs, MnO_2-MWNTs, and PANI/MnO_2-MWNTs at 0.2 A/g in 0.5 M Na_2SO_4 solution

specific capacitance (C_{spec}) for the MWNTs, MnO_2-MWNTs, and PANI/MnO_2-MWNTs can be calculated as:

$$C_{spec} = \frac{I \times t}{\Delta V \times m} \quad (2)$$

where I is the discharge current, m is the electrode mass, t is the discharge time, and ΔV is the voltage range. The C_{spec} (92 F/g) of MWNTs is largely enhanced with the MnO_2 and PANI layer since the C_{spec} values of the MnO_2-MWNTs and PANI/MnO_2-MWNTs are 306 and 350 F/g, respectively. The enhancement of the C_{spec} is attributed to the redox reaction by MnO_2 and nitrogen groups of PANI, and the improved electrochemical performance of the multi-layered electrode

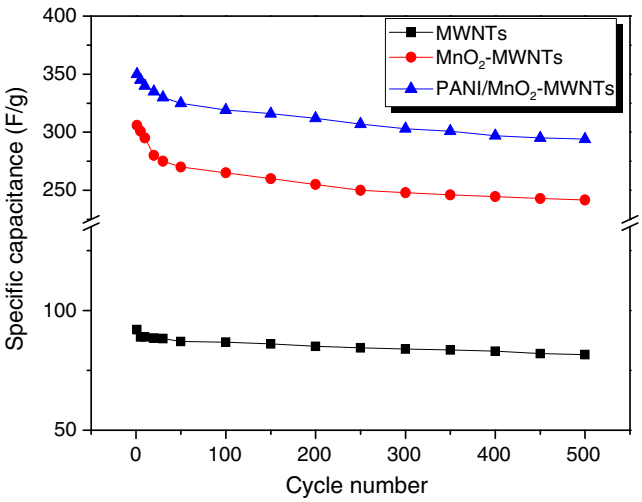

Fig. 9 Specific capacitances of pristine MWNTs, MnO_2-MWNTs, and PANI/MnO_2-MWNTs as a function of cycle number measured at 0.2 A/g in 0.5 M Na_2SO_4 solution

system is mainly related to the nano-scale MnO_2 coating rather than the PANI coating, resulting from the CV curves and charge/discharge results.

Cycle stability of PANI/MnO_2-MWNTs

The long-term cycle stability of each sample, i.e., MWNTs, MnO_2-MWNTs, and PANI/MnO_2-MWNTs, was also evaluated in this study by cycling the charge/discharge test between −0.2 and 1.0 V (vs. Ag/AgCl) at a current density of 0.2 A/g during 500 times. The cycle stability of each sample is shown in Fig. 9. It is obvious that the pristine MWNT-based electrode shows high cycle stability over the entire test period and after 500 cycles, and the capacitance decreased by approximately 7% of the initial capacitance. However, despite the specific capacitance of MnO_2-MWNTs being higher than that of pristine MWNTs, it is gradually decreased with the increasing number of charge–discharge tests, revealing the low cycle stability of about 20%. Previous studies have reported that the reduction of the electrochemical performance of the MnO_2 with cycling is closely related to the physicochemical and structural characteristics, such as grain size, surface area, morphology, and crystallinity [30]. In this system, the gradual decrease of the MnO_2-MWNTs specific capacitance is attributed to the partial dissolution of MnO_2 coated onto MWNTs in the electrolyte during cycling, resulting in an increase of equivalent series resistance at the interface between the electrode materials and current collector [31, 32].

After an additional PANI coating, the PANI/MnO_2-MWNTs exhibit more stable cycle features than the MnO_2-MWNTs where the capacitance decreases by approximately 16 % of the initial capacitance since the PANI layers can reduce the dissolution rate of MnO_2 in the electrolyte solution. It is well known that a combination of MnO_2 and other materials, such as conducting polymers, may reduce both the MnO_2 dissolution and the mechanical failure and hence lead to excellent electrochemical performance after the number of cycling tests [33]. However, the specific capacitance is likewise decreased during the charge/discharge test to an extent that is even greater than that of pristine MWNTs. The decrease of the specific capacitance of the PANI/MnO_2-MWNTs could account for the expansion and shrinkage of the PANI during the long-term charge/discharge processes [34]. Consequently, the nano-scale coated MnO_2 on the MWNTs could provide improved capacitance with higher electric conductivity of MnO_2 as well as enhanced electrolyte migration. The coating of PANI also further improves the electrochemical performance of MnO_2-MWNTs. Therefore, multi-core/shell electrodes are suitable to be manufactured as electrode materials and have superior electrochemical performance when compared to that of conventional manganese oxide/carbon electrodes.

Conclusions

In this work, multi-layered electrodes, i.e., PANI/MnO_2-MWNTs, were prepared as electrode materials for a supercapacitor. The effect of PANI coating on the electrochemical performance and cyclic stability of MnO_2-MWNTs was determined. From the cyclic voltammograms, PANI/MnO_2-MWNTs showed remarkably enhanced specific capacitance and cycle stability compared to pristine MWNTs and MnO_2-MWNTs, and the specific capacitance of PANI/MnO_2-MWNTs (350 F/g) was higher than those of pristine MWNTs (92 F/g) and MnO_2-MWNTs (306 F/g). This indicated that the improved electrochemical performance of PANI/MnO_2-MWNTs was due to the synergistic effect among three components, i.e., PANI, MnO_2, and MWNTs, and the PANI coating resulted in increased cycle stability by delaying the dissolution of MnO_2 during charge/discharge tests.

Acknowledgments This work was supported by the IT Industrial Source Technology Development Business of the Ministry of Knowledge Economy, Korea.

References

1. Conway BE (1999) Electrochemical Supercapacitors. Kluwer Academic, New York
2. Kisacikoglu MC, Uzunoglu M, Alam MS (2009) Int J Hydrogen Energy 34:1497–1507
3. Lim JW, Jeong E, Jung MJ, Lee SI, Lee YS (2012) J Ind Eng Chem 18:116-122
4. Zhang X, Ji L, Zhang S, Yang W (2007) J Power Sources 173:1017–1023
5. Subramanian V, Zhu H, Wei B (2006) Electrochem Commun 8:827–832
6. Kim KS, Park SJ (2011) Electrochim Acta 56:1629–1635
7. Sen P, De A (2010) Electrochim Acta 55:4677–4684
8. Konyushenko EN, Kazantseva NE, Stejskal J, Trchová M, Kovářová J, Sapurina I, Tomishko MM, Demicheva OV, Prokeš J (2008) J Magnetism Magnetic Mater 320:231–240
9. Ma SB, Nam KW, Yoon WS, Yang XQ, Ahn KY, Oh KH, Kim KB (2008) J Power Sources 178:483–489
10. Reddy RN, Reddy RG (2003) J Power Sources 124:330–337
11. Wang Y, Liu H, Sun X, Zhitomirsky I (2009) Scripta Mater 61:1079–1082
12. Long JW, Young AL, Rolison DR (2003) J Electrochem Soc 150: A1161–A1165
13. Fischer AE, Saunders MP, Pettigrew KA, Rolison DR, Long JW (2008) J Electrochem Soc 155:A246–A252
14. Zhang S, Peng C, Ng KC, Chen GZ (2010) Electrochim Acta 55:7447–7453
15. Razak SIA, Ahmad AL, Zeina SHS, Boccaccini AR (2009) Scripta Mater 61:592–595
16. Li D, Kaner RB (2006) J Am Soc Chem 128:968–975
17. Li H, Wang J, Chu Q, Wang Z, Zhang F, Wang S (2009) J Power Sources 190:578–586
18. Kim YY, Yun J, Lee YS, Kim HI (2011) Carbon Lett 12:48-52
19. Lee D, Char K (2002) Polym Degrad Stabil 75:555–560
20. Xie X, Gao L (2007) Carbon 45:2365–2373

21. Chiou NR, Epstein AJ (2005) Adv Mater 17:1679–1683
22. Zheng H, Kang W, Fengming Z, Tang F, Rufford TE, Wang L, Ma C (2010) Solid State Ionics 181:1690–1696
23. Zou W, Wang W, He B, Sun M, Yin Y (2010) J Power Sources 195:7489–7493
24. Djurfors B, Broughton JN, Brett MJ, Ivey DG (2005) Acta Mater 53:957–965
25. Hu CC, Chang KH, Lin MC, Wu YT (2006) Nano Lett 6:2690–2695
26. Sharma RK, Rastogi AC, Desu SB (2008) Electrochim Acta 53:7690–7695
27. Khomenko V, Raymundo-Piñero E, Béguin F (2006) J Power Sources 153:183–190
28. Toupin M, Brousse T, Belanger D (2004) Chem Mater 16:3184–3190
29. Kim S, Park SJ (2008) Anal Chim Acta 619:43–48
30. Brousse T, Toupin M, Dugas R, Athouel L (2006) J Electrochem Soc 153:2171–2180
31. Comaba S, Ogata A, Tsuchikawa T (2008) Electrochem Commun 10:1435–1437
32. Belanger D, Brousse T, Long JW (2008) Electrochem Soc Interf 17:49–52
33. Babakhani B, Ivey DG (2010) J Power Sources 195:2110–2117
34. Khomenko V, Frackowiak E, Beguin F (2005) Electrochim Acta 50:2499–2506